

Analytical and Numerical Studies of Resonant Wave Run-up on a Plane Beach

Erwina, N. *, Erianto, E. S. and Pudjaprasetya, S. R.

Industrial and Financial Mathematics Research Group, Faculty of Mathematics and Natural Sciences, Institut Teknologi Bandung, Indonesia

E-mail: nerwina@math.itb.ac.id

** Corresponding author*

Received: 27 December 2017

Accepted: 16 March 2019

ABSTRACT

Wave run up is the vertical extent of wave up rushed on a beach. In the case of monochromatic wave run-up, it was a common belief that the leading wave will reach the maximum run-up. However, this is not always the case, when the incident wave is of normal mode frequency, resonance phenomena might appear. In this article, the normal mode frequency of a semi-enclosed basin on a plane beach is derived using the variable separation technique. Simulation results demonstrate that when the incoming wave frequency is close to the normal mode frequency, the largest run-up height is not the leading wave, but the second, third or fourth waves, which indicates the occurrence of resonance phenomena. Sensitivity analysis was applied to show the dependence of the maximum run-up height to the beach slope, as well as the incident wave frequency. Further, a simulation using a real bathymetry was conducted to examine whether the resonance phenomenon appears in the actual tsunami events.

Keywords: The Staggered Conservative Scheme, Wave Run-up, Resonance

1. Introduction

Wave run-up on a sloping beach has been studied in the past fifty years. One of challenges in the run-up studies is on coping with moving shoreline. In 1958, an important contribution came from Carrier and Greenspan (1958) which used the hodograph transformation to find analytical solutions of the shallow water equations (SWE). Since then, many researches have used this Carrier and Greenspan transformation to study run-up characteristics of various waves, such as soliton in Kânoğlu and Synolakis (2006), Synolakis (1987), as well as N-wave in Tadepalli and Synolakis (1994). Later, this transformation is also used to study run-up characteristics of monochromatic waves as in Pelinovsky and Mazova (1992) and its relation with surf-similarity parameter as in Madsen and Fuhrman (2008). In 2007, Antuono in Antuono and Brocchini (2007) and Matteo and Brocchini (2008) used this transformation to solve the boundary value problem of SWE in order to find the run-up height formula.

However, most studies on wave run-up do not discuss resonance phenomena, whilst this phenomena may arise in certain situations, namely when the incoming wave frequency is close to beach natural frequency. The occurrence of this phenomena may worsen tsunami impact on beaches. Stefanakis et al. (2011) found that resonance may enhance the run-up of nonleading wave. This causes the run-up height of the following wave is higher than the leading wave. Resonance of long waves on the composite beach was also encountered by Stefanakis et al. (2015), as well as by Ezersky et al. (2013) which includes a discussion of tsunami application.

The staggered conservative scheme as proposed by Stelling and Duinmeijer (2003) is known to be a robust method for simulating various shallow water flows. This scheme can handle simulations involving wet-dry areas. Implementation of this scheme to several test cases, such as transcritical flow and dam break problem can be found in Magdalena et al. (2015), Pudjaprasetya and Magdalena (2014). The main result of this paper is on the direct implementation of the staggered conservative scheme in simulating resonance phenomena of wave run up on a plane beach. The non-dissipative property of the scheme enable us to test the analytically derived natural frequency of the sloping beach system.

Our discussion in this paper is organized as follows. In Section 2, natural frequencies for the semi-enclosed beach is derived analytically. In Section 3, the staggered conservative scheme is reviewed. Run-up height of monochromatic waves and the occurrence of resonance phenomena are investigated in Section 4. Conclusions are given in the last section.

2. Natural Frequency of Long Waves Over a Sloping Beach

In this section we will derive the natural frequency for waves on a plane beach using the variable separation technique. Our discussion start with considering the following linear shallow water equations

$$\eta_t + (d(x)u)_x = 0 \quad (1)$$

$$u_t + g\eta_x = 0 \quad (2)$$

where η is surface elevation, u horizontal velocity, $d(x)$ undisturbed water depth, and g gravitational acceleration. Eliminating u from (1) and (2) will give us

$$\eta_{tt} - (gd(x)\eta_x)_x = 0. \quad (3)$$

Equation (3) is the homogeneous linear wave equation. If we restrict to a beach with a constant slope $\alpha = \tan \theta$, to be explicit $d(x) = -\alpha x$, the equation (3) becomes

$$\eta_{tt} + \alpha g\eta_x + \alpha gx\eta_{xx} = 0. \quad (4)$$

The natural frequency for waves on a plane beach can be obtained via variable separation technique. Next we look for solutions in the form of

$$\eta(x, t) = X(x)e^{-i\omega t} \quad (5)$$

where ω is the wave frequency.

Consider a sloping beach with semi-enclosed boundary condition on a domain $-L \leq x \leq 0$. Using (5), equation (4) reduces to an equation of $X(x)$ reads

$$g\alpha(xX_{xx} + X_x) - \omega^2 X = 0, \quad -L < x < 0. \quad (6)$$

Solutions of (6) are

$$X(x) = C_1 J_0 \left(\sqrt{-\frac{4\omega^2 x}{g\alpha}} \right) + C_2 Y_0 \left(\sqrt{-\frac{4\omega^2 x}{g\alpha}} \right),$$

where J_0 and Y_0 are the zero-th order of the first and second kind of Bessel functions, respectively. Moreover, under the assumption that wave amplitude is bounded, we should have $\lim_{x \rightarrow 0} \eta(x, t)$ is finite. That means the constant C_2 should be zero. For semi enclosed seas connected to the ambient ocean, as recorded by Kämpf (2009), the natural frequency is determined by the normal modes that has a node at the vicinity of the entrance. So, here we adopt

the boundary condition $\eta(-L, t) = 0$, from which we get a relation $X(-L) = C_1 J_0\left(2\sqrt{\frac{\omega^2 L}{g\alpha}}\right) = 0$. Let $2z_k$ be the k -root of $J_0(x)$ on the interval $-L \leq x \leq 0$, to be explicit they read

$$z_1 = 1.2025, \quad z_2 = 2.760, \quad z_3 = 4.3270, \quad \dots \quad (7)$$

Hence, the natural frequency for waves on a plane beach are

$$\omega_k = z_k \sqrt{\frac{g\alpha}{L}}, \quad k = 1, 2, 3, \dots \quad (8)$$

In Section 4 this natural frequency formulas (8) with z_k given in (7) is tested with numerical simulations of wave run-up on a sloping beach. Indeed, for a beach with slope α and length L , incident wave with frequency ω_k will experience oscillation with increasing amplitude.

3. The Staggered Conservative Scheme of SWE

In this section we review the staggered conservative scheme of Stelling and Duinmeijer (2003) that will be used in all simulations conducted in this paper. Consider the following shallow water model, which holds for relatively long waves in a shallow region:

$$h_t + (hu)_x = 0, \quad (9)$$

$$u_t + uu_x + g\eta_x = 0. \quad (10)$$

In the above equations, $u(x, t)$ denotes the depth-averaged horizontal velocity, $h(x, t)$ denotes the total water layer thickness such that $h(x, t) = \eta(x, t) + d(x)$, where $\eta(x, t)$ denotes the free surface elevation and $d(x)$ describes the depth of the bottom topography relative to the undisturbed free surface height, see Figure 1.

On the computational domain $[-L, L]$ which is divided into N_x cells of homogeneous length Δx , a staggered partition points are

$$x_{1/2} = -L, x_{3/2} = \Delta x, \dots, x_{j+1/2} = j\Delta x, \dots, x_{N_x+1/2} = N_x\Delta x = L \quad (11)$$

On this staggered partitions, u are computed on staggered grid, whereas h (which also means η) are computed on full grids, as illustrated in Figure 2.

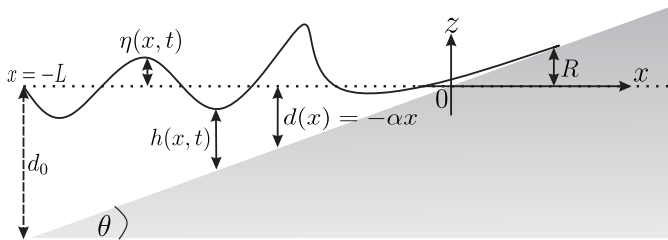


Figure 1: Sketch and notations of wave run-up on a sloping beach.

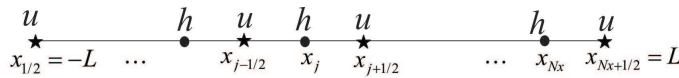


Figure 2: Staggered grid partition of a computational domain $[-L, L]$, with $u_{j+1/2}$ at staggered grid points, and h_j at full grid points.

Here, we consider a staggered conservative scheme for solving the above shallow water equations, for which a discrete formulation of (9,10) is given by

$$\frac{h_i^{n+1} - h_i^n}{\Delta t} = - \left(\frac{{}^*h_{i+\frac{1}{2}}^n u_{i+\frac{1}{2}}^n - {}^*h_{i-\frac{1}{2}}^n u_{i-\frac{1}{2}}^n}{\Delta x} \right) \tag{12}$$

$$\frac{u_{i+\frac{1}{2}}^{n+1} - u_{i+\frac{1}{2}}^n}{\Delta t} = - \frac{1}{\bar{h}_{i+\frac{1}{2}}} \left(\frac{\bar{q}_{i+1} {}^*u_{i+1} - \bar{q}_i {}^*u_i}{\Delta x} - u_{i+\frac{1}{2}} \frac{\bar{q}_{i+1} - \bar{q}_i}{\Delta x} \right) - g \left(\frac{\eta_{i+1}^{n+1} - \eta_i^{n+1}}{\Delta x} \right), \tag{13}$$

respectively. In the above equations

$$\bar{h}_{i+\frac{1}{2}} = \frac{h_i + h_{i+1}}{2}, \quad \bar{q}_i = \frac{q_{i+\frac{1}{2}} + q_{i-\frac{1}{2}}}{2}, \quad q_{i+\frac{1}{2}} = {}^*h_{i+\frac{1}{2}} u_{i+\frac{1}{2}}.$$

Upwind approximations for *h and *u are given by

$${}^*h_{i+\frac{1}{2}} = \begin{cases} h_i, & \text{if } u_{i+\frac{1}{2}}^n \geq 0, \\ h_{i+1}, & \text{if } u_{i+\frac{1}{2}}^n < 0, \end{cases} \quad {}^*u_i = \begin{cases} u_{i-\frac{1}{2}}, & \text{if } \bar{q}_i \geq 0, \\ u_{i+\frac{1}{2}}, & \text{if } \bar{q}_i < 0. \end{cases} \tag{14}$$

For simulation of wave over a sloping beach, the numerical scheme should be able to accommodate wet-dry region. Here the wet-dry procedure is simply, computing the discrete formula (13) only if the water depth at the momentum cell $[x_{j-1/2}, x_{j+1/2}]$ is greater than a minimum threshold depth h_{min} . Ideally,

this threshold depth h_{min} is zero, but to avoid computation difficulties of division using small number, we often need to adopt $h_{min} \approx 10^{-2}$, or other small number depending on the particular problem we are dealing with. By adopting this simple requirement, the staggered scheme (12, 13) can handle simulations that involve dry areas. A more detailed discussion of this staggered scheme can be seen in Pudjaprasetya and Magdalena (2014), Stelling and Zijlema (2003), Stelling and Duinmeijer (2003).

3.1 Simulation of wave oscillation over a sloping beach

In this section, the staggered scheme (12, 13) is implemented on a computational domain $[-L, L]$, to simulate waves run-up over a sloping topography $d(x) = -\alpha x$. Sketch of notations and variables are depicted in Figure 1.

Our simulation use the initial still water level and the following parameters $L = 12.5 \text{ m}$, $\alpha = 0.13$, and gravitational acceleration $g = 9.81 \text{ m/s}^2$. Further, we employ a monochromatic wave influx that enters from the left by taking

$$\eta(-L, t) = \eta_0 \sin \omega t, \quad (15)$$

where η_0 and ω denote wave amplitude and frequency, respectively. Computation were conducted using $\Delta x = 0.1 \text{ m}$, and $\Delta t = \frac{\Delta x}{2\sqrt{gd_0}} = 0.0124 \text{ s}$, to maintain stability. This first simulation uses $\eta_0 = 0.025 \text{ m}$, and $\omega = 0.6 \text{ s}^{-1}$, snapshots of surface wave at subsequent times are given in Figure 3.

As depicted in Figure 1, the vertical extend of shoreline during run up process is denoted as R , whereas R_{max} denotes its maximum run up. When shoreline position of the previous simulation, is recorded, the result is plotted on Figure 4 (top). From the inset figure we can observe that the leading wave hit the shoreline and reach the vertical extent of $R/\eta_0 = 4.68$. Wave up rush to the sloping beach is followed with wave run-down. As time progresses, this run-up and run-down process is continued. We observed that the following run up height is less than the first run up by the leading wave. The second run up height is $R/\eta_0 = 4.16$. In this numerical experiment the maximum run up is the fifth run up with $R/\eta_0 = 5.2$. In most simulations, the maximum run up height is achieved by the first wave. However, when the resonance takes place, run up of the second wave is larger, and run up of the third or later waves may even larger.

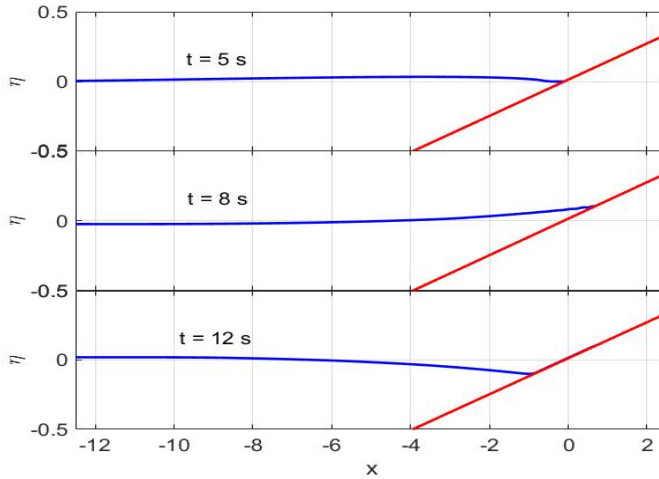


Figure 3: Snapshot of surface profile $\eta(x, t)$ at subsequent times.

4. Resonance on a Plane Beach

Under the same set up like the previous, $L = 12.5 \text{ m}$, $\alpha = 0.13$, and $\eta_0 = 0.025 \text{ m}$, but now we conduct a simulation using monochromatic wave influx (15) with frequency $\omega = 0.4 \text{ s}^{-1}$. This time the frequency of the wave influx matches with the natural frequency ω_1 as in (8). Shoreline position as a function of time was recorded, and the result is given in Figure 4 (bottom). This shoreline motion clear show that this time the wave influx gives rise to a resonance phenomenon. As shown in Figure 4 that while run up height of wave $\omega = 0.6 \text{ s}^{-1}$ remains within the normal range of $\frac{R}{\eta_0} \in [-4.16, 5.20]$, run up height of wave $\omega = 0.4 \text{ s}^{-1}$ exhibits resonance behavior: its value is increases from the first wave, the second and so on. This value continues to increase until the seventh wave that reaches the maximum of $\frac{R_{max}}{\eta_0} = 27.04$, which then slightly decreases afterwards. Thus, resonance phenomenon is clearly observable in the case of wave oscillation over a sloping beach with $\omega = 0.4 \text{ s}^{-1}$.

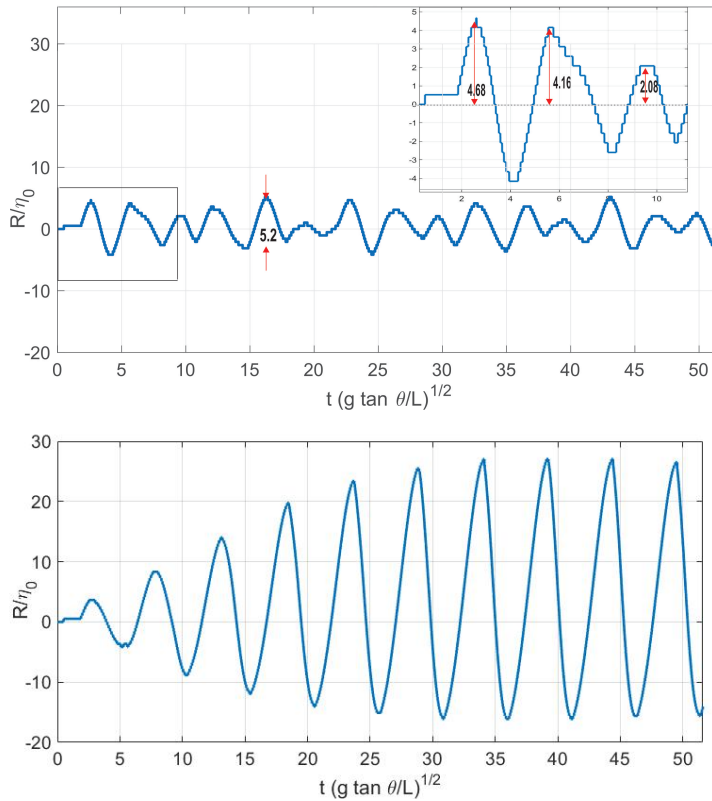


Figure 4: Plot of wave run-up R/η_0 as a function of time for beach with slope $\alpha = 0.13$ with wave frequency (top) $\omega = 0.6 \text{ s}^{-1}$, (bottom) $\omega = 0.4 \text{ s}^{-1}$.

Further, for both cases $\omega = 0.4 \text{ s}^{-1}$ and $\omega = 0.6 \text{ s}^{-1}$, we compute the total fluid volume $V = \int h \, dx$ as time progresses. It is shown in Figure 5 that indeed in the case of resonance, the total volume increases as time progresses, which means more and more fluid involve in the oscillation. Whereas in the case of non-resonance, the total fluid volume remains about the same as the initial volume V_0 up to 5% accuracy.

Resonant Wave Run-up on a Plane Beach

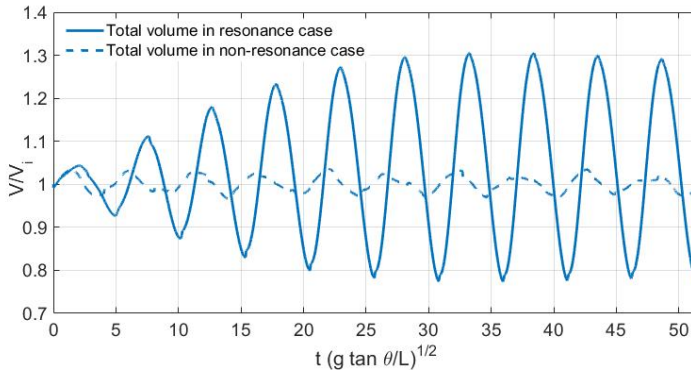


Figure 5: Total fluid volume as time progresses in the case of resonance versus non-resonance

Moreover, total energy of the system is also computed. Here total energy is defined as the sum of potential energy E_p and kinetic energy E_k as follows

$$E_p = \frac{1}{2} \rho g \int_x \eta^2 dx, \quad (16)$$

$$E_k = \frac{1}{2} \rho \int_x hu^2 dx. \quad (17)$$

In the non-resonance case, the computed total energy remains constant, whereas in the case of resonance, the kinetic energy E_k is oscillating with increasing amplitude. This increase in amplitude occurs as time progresses, but after sometime it slightly decreases. Something similar applies to the potential energy E_p , which means it applies to the total energy $E_k + E_p$ as well, see Figure 6.

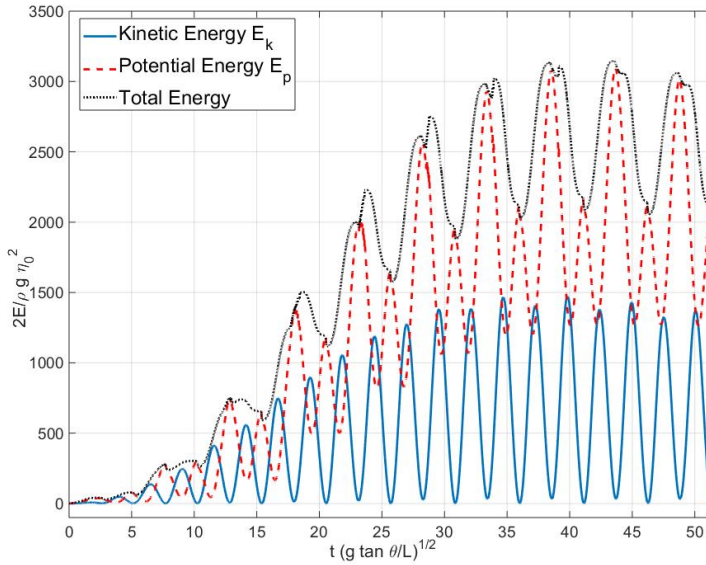


Figure 6: Plot of kinetic energy E_k , potential energy E_p , and total energy of the system as functions of time the case of resonance.

4.1 Maximum run up

In this section, we study the dependence of maximum run-up with respect to wave frequency, and the beach slope.

For this study, three beach slopes were used, i.e. $\alpha = 0.13, 0.26, 0.3$, with the same beach length $L = 12.5 \text{ m}$. For each slope, we conduct simulations using various wave frequency. For every beach slope, run up height R of each wave frequency ω is measured, and the result is plotted in Figure 7. In Figure 7 the maximum run up is plotted with respect to the normalized frequency $z = \omega/(g\alpha/L)^{1/2}$. It is shown that for all three slopes $\alpha_1 = 0.13$, $\alpha_2 = 0.26$, and $\alpha_3 = 0.3$, the first amplification of maximum run up is achieved at the first normalized frequency 1.2, followed by the second and third amplification that achieved at 2.8 and 4.4, respectively. Our numerical results clearly confirm the analytical formula of the normalized frequency as derived in Section 2, which is half of the zeroes of the Bessel function J_0 as provided in (7).

Resonant Wave Run-up on a Plane Beach

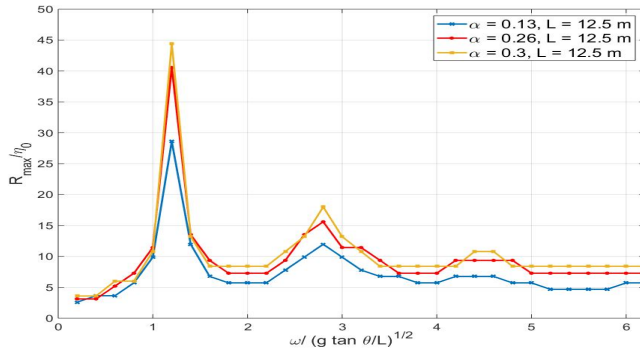


Figure 7: Maximum run-up versus normalized frequency $z = \omega/\sqrt{\frac{g\alpha}{L}}$.

Further, the dependence of run-up height R_{\max}/η_0 to λ_0 is studied by the following sensitivity analysis. In Figure 8 the maximum run up is plotted against the normalized wave length λ_0/L , where λ_0 is associated to ω through the shallow water relation

$$\frac{2\pi}{\lambda_0} \sqrt{gL\alpha} = \omega \quad \text{or} \quad \frac{\lambda_0}{L} = \frac{2\pi}{\omega} \sqrt{\frac{g\alpha}{L}}.$$

Several simulations with various wave length λ_0 of monochromatic wave were conducted for beaches with three different slopes $\alpha = 0.13, 0.26$ dan 0.3 . The highest value for the maximum wave run-up occur when $\lambda_0/L = 5$. Another high run up value is achieved when $\lambda_0/L = 2$.

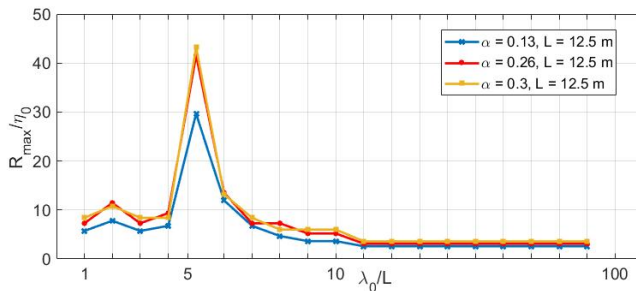


Figure 8: Maximum run-up versus normalized wave length λ_0/L

4.2 Wave run-up on Mentawai beach

In this section we use real data to study whether similar resonant occur during real tsunami. We consider the Mentawai Island tsunami on October 25th 2010. Following Stefanakis et al. (2011) approach, here we use a tsunami influx from a virtual wave-gage located at Lon = 100.24⁰E, Lat = -3.4⁰N, on the water depth 120 *m* of a plane beach with slope $\alpha = 0.03$. Note that this slope is a good approximation of the actual topography near the location of the wave-gage. Simulation is conducted using our staggered numerical scheme, and run up height is measured and the result is plotted in Figure 9. It is shown that our result is nicely comparable with Stefanakis et al. (2011). The simulated shoreline position as plotted in Figure 9 show that the highest run up is achieved not by the leading wave, but by the third wave. This simple observation suggests that similar resonant phenomena may occur during real tsunami.

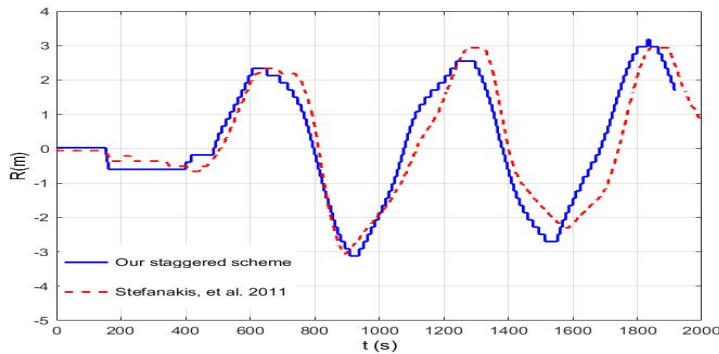


Figure 9: Run up height during the first 2000 s on Mentawai beach, computed using our staggered scheme (solid) and the finite volume characteristic flux scheme by Stefanakis (dashed).

Acknowledgement

Financial support from DIKTI Research Grant No. 534i/II.C01/PL/2018 is gratefully acknowledged.

References

Antuono, M. and Brocchini, M. (2007). The boundary value problem for the nonlinear shallow water equations. *Studies in Applied Mathematics*,

119(1):73–93.

- Carrier, G. F. and Greenspan, H. P. (1958). Water waves of finite amplitude on a sloping beach. *Journal of Fluid Mechanics*, 4(1):97–109.
- Ezersky, A., Abcha, N., and Pelinovsky, E. (2013). Physical simulation of resonant wave run-up on a beach. *Nonlinear Processes in Geophysics*, 20(1):35–40.
- Kämpf, J. (2009). *Ocean Modelling for Beginners*. Springer.
- Kanoğlu, U. and Synolakis, C. (2006). Initial value problem solution of nonlinear shallow water-wave equations. *Phys. Rev. Lett.*, 97:148–501.
- Madsen, P. A. and Fuhrman, D. R. (2008). Run-up of tsunamis and long waves in terms of surf-similarity. *Coastal Engineering*, 55:209–223.
- Magdalena, I., Erwina, N., and Pudjaprasetya, S. R. (2015). Staggered momentum conservative scheme for radial dam break simulation. *J. Sci. Comput.*, 65(3):867–874.
- Matteo, A. and Brocchini, M. (2008). Maximum run-up, breaking conditions and dynamical forces in the swash zone: a boundary value approach. *Coastal Engineering*, 55(9):732 – 740.
- Pelinovsky, E. N. and Mazova, R. K. (1992). Exact analytical solutions of nonlinear problems of tsunami wave run-up on slopes with different profiles. *Natural Hazards*, 6:227–249.
- Pudjaprasetya, S. R. and Magdalena, I. (2014). Momentum conservative schemes for shallow water flows. *East Asian Journal on Applied Mathematics*, 4(2):152–165.
- Stefanakis, T. S., Dias, F., and Dutykh, D. (2011). Local run-up amplification by resonant wave interactions. *Phys. Rev. Lett.*, 107:124–502.
- Stefanakis, T. S., Xu, S., , and Dutykh, D. (2015). Run-up amplification of transient long waves. *Quarterly of Applied Mathematics*, 123(1):177–199.
- Stelling, G. and Zijlema, M. (2003). An accurate and efficient finite-difference algorithm for non-hydrostatic free-surface flow with application to wave propagation. *International Journal for Numerical Methods in Fluids*, 43(1):1–23.
- Stelling, G. S. and Duijnmeijer, S. P. A. (2003). A staggered conservative scheme for every froude number in rapidly varied shallow water flows. *International Journal for Numerical Methods in Fluids*, 43(12):1329–1354.

Erwina, N., Erianto, E. S. & Pudjaprasetya, S. R.

Synolakis, C. E. (1987). The runup of solitary waves. *Journal of Fluid Mechanics*, 185:523–545.

Tadepalli, S. and Synolakis, C. E. (1994). The run-up of n-waves on sloping beaches. *Proceedings of the Royal Society of London A: Mathematical, Physical and Engineering Sciences*, 445(1923):99–112.